

NUMERICAL SOLUTION OF FOURTH ORDER GENERALISED KURAMOTO-SIVASHINSKY EQUATION USING MODIFIED QUINTIC B-SPLINE DIFFERENTIAL QUADRATURE METHOD

NUMERIČKO REŠENJE GENERALISANE JEDNAČINE ČETVRTOG REDA KURAMOTO-SIVASHINSKY PRIMENOM MODIFIKOVANE PETOSTEPENE B-SPLAJN DIFERENCIJALNE METODE KVADRATURE

Originalni naučni rad / Original scientific paper

Rad primljen / Paper received: 15.07.2024

<https://doi.org/10.69644/ivk-2025-siA-0057>

Adresa autora / Author's address:

¹ Department of Mathematics, School of Advanced Sciences, Vellore Institute of Technology, Vellore, Tamil Nadu, India
*email: rachna.bhatia@vit.ac.in

² University of Niš, Faculty of Sciences and Mathematics, Niš, Serbia

Keywords

- modified quintic B-spline
- differential quadrature method
- extended Fisher-Kolmogorov equation
- Kuramoto-Sivashinsky equation
- matrix stability method

Abstract

In this paper, numerical solutions of the nonlinear generalised Kuramoto-Sivashinsky equation are presented using a modified quintic B-spline differential quadrature method. The Crank-Nicolson and forward finite difference schemes are applied for discretization, while the Rubin and Graves approach is utilised for linearization. The matrix stability approach is used to analyse the method's stability. Numerical examples demonstrate the accuracy of the method. The computed results are presented in tables and graphs along with a comparative analysis with previous results. The obtained numerical results demonstrate the method's reliability and its compatibility with the exact solutions.

INTRODUCTION

A fourth order partial differential equation known as the Generalised Kuramoto-Sivashinsky (GKS) equation characterizes the spatiotemporal evolution of the amplitude of coherent structures in specific nonlinear systems. It has found applications in various fields, including physics, chemistry, and fluid dynamics. The GKS equation has been used to investigate the dynamics of flame fronts in combustion processes. Comprehending the progression of flame fronts is essential for optimising combustion effectiveness and managing pollutants. It can also be used to simulate the surface growth of thin films or crystal growth in materials science. This equation is important for studying turbulent flows, because it helps to explain the dynamics and generation of coherent structures in turbulent boundary layers. The GKS equation have been used to describe the evolution of concentration patterns which can be used to explore pattern development in a variety of systems, including chemical reactions. Certain biological phenomena, such as the dynamics of spatial patterns in reaction-diffusion systems within biological tissues, can be modelled using the GKS equation. The GKS equation can be used to model chemical kinetics, particularly when reaction and diffusion processes interact

Ključne reči

- modifikovan petostepeni B-splajn
- metoda diferencijalne kvadrature
- proširena jednačina Fišer-Kolmogorov
- jednačina Kuramoto-Sivashinsky
- metoda stabilne matrice

Izvod

U radu su predstavljena numerička rešenja nelinearne generalisane jednačine Kuramoto-Sivashinsky, primenom modifikovane diferencijalne metode kvadrature petostepenog B-splajna. Primenjuje se postupak Krank-Nikolson sa konačnom razlikom unapred za diskretizaciju, dok se pristup Rubina i Grejvsa koristi za linearizaciju. Metoda stabilne matrice se koristi za analizu stabilnosti korišćene metode. Numerički primeri pokazuju tačnost metode. Izračunati rezultati su predstavljani tabelarno i grafički sa uporednom analizom ranijih rezultata. Dobijeni numerički rezultati ukazuju na pouzdanost korišćene metode i na poklapanje sa tačnim rešenjima.

to create spatial patterns. These applications demonstrate applicability of GKS equation to a variety of scientific and engineering fields to describe a broad range of complex phenomena. In this paper we consider the following GKS equation:

$$U_t + \alpha U U_x + \beta U_{xx} + \gamma U_{xxx} + \mu U_{xxxx} + g(U) = 0 \quad (1)$$

The Eq.(1) frequently lacks analytical solutions for general situations due to the presence of nonlinearity and up to fourth-order partial derivatives. Therefore, numerical solutions are essential to examine its behaviour in practical situations. Many well-known equations can be obtained by changing the values of real constants and nonlinear function $g(U)$. The following high order PDEs (PDEs involving third and fourth order derivatives) are taken into consideration as specific cases of the generalised equation mentioned above.

Extended Fisher-Kolmogorov equation

The spatial and temporal evolution of populations is commonly explained by the Extended Fisher-Kolmogorov (EFK) equation, which has applications in the fields of population biology and ecology. Coulet et al. /7/ and Van Saarloos /10/ introduced this equation. EFK arises from the usage of particular values $\alpha = \gamma = 0$, $\beta = -1$, and $g(U) = U^3 - U$ in Eq.(1),

$$U_t - U_{xx} + \mu U_{xxxx} + g(U) = 0 \quad (2)$$

Equation (2) reduces to the standard form of the Fisher-Kolmogorov equation by the replacement $\mu = 0$.

Researchers have concentrated on examining the equation's steady state which is based on μ and exhibits periodic solutions that are either heteroclinic or homoclinic. There are two types of solution behaviours for the EFK equation, depending on μ . In the case $\mu > 1/8$, the solution is non-monotonic, and for $\mu \leq 1/8$, it is both unique and exists. Using the shooting method, Peletier and Troy in /26, 27/ investigate the solution in a steady state. A simple lower bound on the fronts' velocities is found by Benguria and Depassier /5/ to aid in predicting when the front with the lowest speed will be pushed for a particular reaction term. Zuo /32/ proposed two high-order compact finite difference schemes to solve the EFK equation. Using a variety of numerical techniques, numerous researchers have provided solutions to this equation in recent years. A fully discrete Galerkin approximation has been developed by Gudi and Gupta /11/.

Kuramoto-Sivashinsky equation

Applications of the Kuramoto-Sivashinsky (KS) equation is available in many scientific and engineering fields where an understanding of turbulence, pattern formation, and non-linear dynamics is essential to the explanation of complex phenomena. Equation (1) in the case of vanishing nonlinear term $g(U) = 0$ turns into the following KS equation

$$U_t + \alpha U U_x + \beta U_{xx} + \gamma U_{xxx} + \mu U_{xxxx} = 0. \tag{3}$$

Turbulence and complex pattern creation are greatly aided by the nonlinear term $U U_x$ in Eq.(3). Numerous scholars have worked with this equation and developed exact and numerical methods. Some of them are: a moving least squares meshless method /9/, B-spline function based collocation method /18/, meshless method of lines /12/, quintic B-spline collocation method /24/, a modified tanh-coth method /30/, lattice Boltzmann method /17/, a time-adaptive finite volume method /8/, Chebyshev spectral collocation methods /16/, local discontinuous Galerkin methods /31/, implicit-explicit BDF methods /1/, quartic-trigonometric tension B-spline /13/.

Partial differential equations have been frequently solved numerically using B-splines in combination with the collocation method /19, 20/ and differential quadrature methods /6, 21/. Mittal and Dahiya /22/ described a quintic B-spline based differential quadrature method for a class of Fisher-Kolmogorov equations. Ismail et al. /14/ developed three-level linearized high-order accuracy difference scheme. Since Differential Quadrature Method (DQM) commonly yields high accuracy solutions and frequently needs fewer grid points to attain equivalent accuracy than finite difference or finite element approaches. The combination of B-splines with DQM yield a numerical solution that benefits from both DQM's precision and B-splines' smoothness. As a result, the PDE solution approximations become more precise.

In this paper, modified quintic B-spline functions and DQM are combined to approximate solutions of Kuramoto-Sivashinsky (KS) equation and extended Fisher-Kolmogorov (EFK) equation. The following section presents the DQM based on modified quintic B-spline functions. The further section presents a numerical scheme. Then we discuss the

scheme's stability analysis and give a validation of presented numerical scheme considered by examples. Finally, we give the final conclusions.

MODIFIED DQM SUPPORTED BY QUINTIC B-SPLINE

The DQM was first introduced by Bellman et al. /3/. This method involves the technique of approximating derivatives of a function at certain grid points using the weighted sum of functional values. These weighting coefficients only depend on the spatial grid spacing.

Several test functions, including spline functions, Lagrange interpolated cosine functions, Legendre polynomials, Lagrange interpolation polynomials, and others, have been used by numerous authors to develop various types of DQMs /3, 4, 28, 29/. DQM offers a significant advantage over traditional approaches since it avoids perturbations for obtaining better solutions to the nonlinear PDEs. Its broad applicability, simple execution, and easy-to-understand concepts make it an advantage over other approaches.

Let us consider N uniform grid points x_1, \dots, x_N within a finite interval $[a_1, a_2]$ on the real axis, and assume $a_1 = x_1 < x_2 < x_3 < \dots < x_N = a_2$ with $h = x_{(i+1)} - x_{(i)}$. Using DQM, the n^{th} order derivative of a function $U(x,t)$ at a point x_i can be approximated by the rule

$$U_x^{(n)}(x_i, t) = \sum_{j=1}^N w_{ij}^{(n)} U(x_j, t) \quad i = 1 \dots N, n = 1 \dots N-1, \tag{4}$$

in which $w_{ij}^{(n)}$ are unknown weighting coefficients of the n^{th} order derivative.

The uniform quintic B-spline functions $R_i(x)$ are uniformly distributed over the interval $[a_1, a_2]$ and B-splines consisting of $\{R_{-1}, R_0, R_1, \dots, R_{N+2}\}$ form a basis over the interval $[a_1, a_2]$. The quintic B splines $R_i(x)$ are given by

$$R_i(x) = \frac{1}{h^5} \begin{cases} (x - x_{i-3})^5, & x \in [x_{i-3}, x_{i-2}), \\ (x - x_{i-3})^5 - 6(x - x_{i-2})^5, & x \in [x_{i-2}, x_i), \\ (x - x_{i-3})^5 - 6(x - x_{i-2})^5 + 15(x - x_{i-1})^5, & x \in [x_{i-1}, x_i), \\ (x_{i+3} - x)^5 - 6(x_{i+2} - x)^5 + 15(x_{i+1} - x)^5, & x \in [x_i, x_{i+1}), \\ (x_{i+3} - x)^5 - 6(x_{i+2} - x)^5, & x \in [x_{i+1}, x_{i+2}), \\ (x_{i+3} - x)^5, & x \in [x_{i+2}, x_{i+3}), \\ 0, & \text{otherwise} \end{cases}$$

Quintic B-splines and their derivatives are given in Table 1 for different grid points.

Table 1. Quintic B-splines and its derivatives at different grid points.

	x_{i-3}	x_{i-2}	x_{i-1}	x_i	x_{i+1}	x_{i+2}	x_{i+3}
$R_i(x)$	0	1	26	66	26	1	0
$R_i^{(1)}(x)$	0	5/h	50/h	0	-50/h	-5/h	0
$R_i^{(2)}(x)$	0	20/h ²	40/h ²	-120/h ²	40/h ²	20/h ²	0
$R_i^{(3)}(x)$	0	60/h ³	-120/h ³	0	120/h ³	-60/h ³	0
$R_i^{(4)}(x)$	0	120/h ⁴	-480/h ⁴	720/h ⁴	-480/h ⁴	120/h ⁴	0

When quintic B-splines are used as the test functions in DQM, a total of four ghost points are introduced outside the boundary, two on the left and two on the right hand side. If these ghost points are directly used in DQM to compute weighing coefficients, additional weighting coefficients appear

$$\beta_{N-1}^{(1)} = [w_{N-1,1}^{(1)}, w_{N-1,2}^{(1)}, w_{N-1,3}^{(1)}, \dots, w_{N-1,N-1}^{(1)}, w_{N-1,N}^{(1)}]^T,$$

$$\gamma_{N-1}^{(1)} = \left[0, \dots, 0, \frac{-5}{h}, \frac{-50}{h}, \frac{-5}{h}, \frac{60}{h} \right]^T.$$

Finally, the following situation appears at $x = x_N$,

$$\beta_N^{(1)} = [w_{N,1}^{(1)}, w_{N,2}^{(1)}, w_{N,3}^{(1)}, \dots, w_{N,N-1}^{(1)}, w_{N,N}^{(1)}]^T,$$

$$\gamma_N^{(1)} = \left[0, \dots, 0, \frac{-5}{h}, \frac{-110}{h}, \frac{-115}{h} \right]^T.$$

The same process can be used to derive the weighting coefficients for higher order derivatives.

NUMERICAL SCHEME

The GKS equation is discretized using Crank Nicolson and forward finite difference method Eq.(1) as follows:

$$\frac{U^{n+1} - U^n}{\Delta t} + \alpha \frac{(UU_x)^{n+1} + (UU_x)^n}{2} + \beta \frac{U_{2x}^{n+1} + U_{2x}^n}{2} + \gamma \frac{U_{3x}^{n+1} + U_{3x}^n}{2} + \mu \frac{U_{4x}^{n+1} + U_{4x}^n}{2} + \frac{(g(U))^{n+1} + (g(U))^n}{2} = 0. \quad (7)$$

Rewriting Eq.(7) by separating the $(n+1)^{th}$ and n^{th} time levels, it can be obtained

$$2U^{n+1} + \Delta t(\alpha(UU_x)^{n+1} + \beta U_{2x}^{n+1} + \gamma U_{3x}^{n+1} + \mu U_{4x}^{n+1}) + \Delta t(g(U))^{n+1} = 2U^n - \Delta t(\alpha(UU_x)^n + \beta U_{2x}^n + \gamma U_{3x}^n + \mu U_{4x}^n + (g(U))^n).$$

Linearization of KS equation

Consider the KS equation

$$U_t + \alpha UU_x + \beta U_{xx} + \gamma U_{xxx} + \mu U_{xxxx} = 0. \quad (8)$$

The nonlinear term UU_x in Eq.(8) is linearized using the

$$(UU_x)^{n+1} = U^{n+1}U_x^n + U^nU_x^{n+1} - U^nU_x^n, \quad (9)$$

$$(UU_x)^n = U^nU_x^n.$$

Substituting Eq.(9) in Eq.(7) and rearranging the terms at $(n+1)^{th}$ and n^{th} time levels, leads to the system

$$2U^{n+1} + \Delta t[\alpha(U^{n+1}U_x^n + U^nU_x^{n+1}) + \beta U_{2x}^{n+1} + \gamma U_{3x}^{n+1} + \mu U_{4x}^{n+1}] = 2U^n - \Delta t[\beta U_{2x}^n + \gamma U_{3x}^n + \mu U_{4x}^n].$$

Now, partial order derivatives of U are approximated using modified DQM at the grid point $x = x_i$ at the n^{th} time, the partial orders are denoted as follows:

$$A_i^n = U_x^n(x = x_i), \quad B_i^n = U_{xx}^n(x = x_i), \quad C_i^n = U_{xxx}^n(x = x_i), \quad D_i^n = U_{xxxx}^n(x = x_i).$$

The following system is obtained by reorganising the terms for each grid point:

$$(2 + \Delta t[\alpha(A_i^n + U_i^n w_{ii}^{(1)}) + \beta w_{ii}^{(2)} + \gamma w_{ii}^{(3)} + \mu w_{ii}^{(4)}])U_i^{n+1} + \sum_{j=1, i \neq j}^N \Delta t[\alpha(U_i^n w_{ij}^{(1)}) + \beta w_{ij}^{(2)} + \gamma w_{ij}^{(3)} + \mu w_{ij}^{(4)}]U_j^{n+1} = \Phi_i^n \quad (10)$$

where: $\Phi_i^n = 2U_i^n - \Delta t[\beta B_i^n + \gamma C_i^n + \mu D_i^n]$, for $i = 1, 2, \dots, N$.

Finally, after applying the boundary conditions to the system of Eqs.(10), the first and last equations get eliminated yielding the system

$$\begin{bmatrix} Q_{2,2} & Q_{2,3} & \dots & Q_{2,N-1} \\ Q_{3,2} & Q_{3,3} & \dots & Q_{3,N-1} \\ \vdots & \vdots & \ddots & \vdots \\ Q_{N-2,2} & Q_{N-2,3} & \dots & Q_{N-2,N-1} \\ Q_{N-1,2} & Q_{N-1,3} & \dots & Q_{N-1,N-1} \end{bmatrix} \begin{bmatrix} U_2^{n+1} \\ U_3^{n+1} \\ \vdots \\ U_{N-2}^{n+1} \\ U_{N-1}^{n+1} \end{bmatrix} =$$

$$= \begin{bmatrix} \Phi_2^n - Q_{2,1} U_1^{n+1} - Q_{2,N} U_N^{n+1} \\ \Phi_3^n - Q_{3,1} U_1^{n+1} - Q_{3,N} U_N^{n+1} \\ \vdots \\ \Phi_{N-2}^n - Q_{N-2,1} U_1^{n+1} - Q_{N-2,N} U_N^{n+1} \\ \Phi_{N-1}^n - Q_{N-1,1} U_1^{n+1} - Q_{N-1,N} U_N^{n+1} \end{bmatrix}, \quad (11)$$

in which

$$Q_{i,i} = 2 + \Delta t[\alpha(A_i^n + U_i^n w_{ii}^{(1)}) + \beta w_{ii}^{(2)} + \gamma w_{ii}^{(3)} + \mu w_{ii}^{(4)}],$$

$$Q_{i,j} = \Delta t[\alpha(U_i^n w_{ij}^{(1)}) + \beta w_{ij}^{(2)} + \gamma w_{ij}^{(3)} + \mu w_{ij}^{(4)}].$$

The solution $U(x,t)$ of the system of Eqs.(11) is obtained by the Gauss elimination process.

Linearization of EFK equation

Consider the EFK equation

$$U_t - U_{xx} + \mu U_{xxxx} + (U^3 - U) = 0. \quad (12)$$

The nonlinear term U^3 in Eq.(12) is linearized by the Rubin and Graves technique as follows:

$$(U^3)^{n+1} = 3U^{2(n)} U^{n+1} - 2U^{3(n)}.$$

Now, the above equation is substituted in Eq.(7) and then n^{th} and $(n+1)^{th}$ term are arranged separately, as follows

$$2U^{n+1} + \Delta t[\mu U_{4x}^{n+1} - U_{2x}^{n+1} + 3U^{2(n)}U^{n+1} - U^{n+1}] = 2U^n - \Delta t[\mu U_{4x}^n - U_{2x}^n - U^{3(n)} - U^n].$$

The following system is obtained after approximating partial order derivatives

$$(2 + \Delta t[\mu w_{ii}^{(4)} - w_{ii}^{(2)} + 3U_i^{2(n)} - 1])U_i^{n+1} + \sum_{j=1, i \neq j}^N \Delta t[\mu w_{ij}^{(4)} - w_{ij}^{(2)}]U_j^{n+1} = \Phi_i^n, \quad (13)$$

where: $\Phi_i^n = 2U_i^n - \Delta t[\mu D_i^n - B_i^n - U_i^{3(n)} - U_i^n]$, for $i = 1 \dots N$.

Finally, after applying boundary conditions to the system of equations, a similar system of equations is obtained as in Eqs.(11), in which

$$Q_{i,i} = 2 + \Delta t[\mu w_{ii}^{(4)} - w_{ii}^{(2)} + 3U_i^{2(n)} - 1],$$

$$Q_{i,j} = \Delta t[\mu w_{ij}^{(4)} - w_{ij}^{(2)}].$$

The system of Eqs.(11) is solved utilising the Gauss elimination, and the solution $U(x,t)$ is obtained.

STABILITY ANALYSIS

Stability analysis of the proposed method is investigated using the matrix stability method, /15/.

Consider the linearized KS equation in Eq.(10). It is simplified as follows

$$(2 + \Delta t[\alpha(A_i^n + U_i^n w_{ii}^{(1)}) + \beta w_{ii}^{(2)} + \gamma w_{ii}^{(3)} + \mu w_{ii}^{(4)}])U_i^{n+1} + \sum_{j=1, i \neq j}^N \Delta t[\alpha(U_i^n w_{ij}^{(1)}) + \beta w_{ij}^{(2)} + \gamma w_{ij}^{(3)} + \mu w_{ij}^{(4)}]U_j^{n+1} = (2 - \Delta t[\beta w_{ii}^{(2)} + \gamma w_{ii}^{(3)} + \mu w_{ii}^{(4)}])U_i^n - \sum_{j=1, i \neq j}^N \Delta t[\beta w_{ij}^{(2)} + \gamma w_{ij}^{(3)} + \mu w_{ij}^{(4)}]U_j^n + L_i, \quad (14)$$

such that L_i is the non-homogeneous part along with boundary conditions. The above systems of linear algebraic equations can be stated in the matrix form

$$\begin{bmatrix} G_{2,2} & G_{2,3} & \dots & G_{2,N-1} \\ G_{3,2} & G_{3,3} & \dots & G_{3,N-1} \\ \vdots & \vdots & \ddots & \vdots \\ G_{N-2,2} & G_{N-2,3} & \dots & G_{N-2,N-1} \\ G_{N-1,2} & G_{N-1,3} & \dots & G_{N-1,N-1} \end{bmatrix} \begin{bmatrix} U_2^{n+1} \\ U_3^{n+1} \\ \vdots \\ U_{N-2}^{n+1} \\ U_{N-1}^{n+1} \end{bmatrix} =$$

$$= \begin{bmatrix} S_{2,2} & S_{2,3} & \dots & S_{2,N-1} \\ S_{3,2} & S_{3,3} & \dots & S_{3,N-1} \\ \vdots & \vdots & \ddots & \vdots \\ S_{N-2,2} & S_{N-2,3} & \dots & S_{N-2,N-1} \\ S_{N-1,2} & S_{N-1,3} & \dots & S_{N-1,N-1} \end{bmatrix} \begin{bmatrix} U_2^n \\ U_3^n \\ \vdots \\ U_{N-2}^n \\ U_{N-1}^n \end{bmatrix} + \mathbf{L}, \quad (15)$$

in which \mathbf{L} is a known $(N-2) \times 1$ vector, \mathbf{G} is an invertible matrix, and

$$\begin{aligned} G_{ii} &= 2 + \Delta t [\alpha (A_i^n + U_i^n w_{ii}^{(1)}) + \beta w_{ii}^{(2)} + \gamma w_{ii}^{(3)} + \mu w_{ii}^{(4)}], \\ G_{ij} &= \Delta t [\alpha (U_i^n w_{ij}^{(1)}) + \beta w_{ij}^{(2)} + \gamma w_{ij}^{(3)} + \mu w_{ij}^{(4)}], \\ S_{ii} &= 2 - \Delta t [\beta w_{ii}^{(2)} + \gamma w_{ii}^{(3)} + \mu w_{ii}^{(4)}], \\ S_{ij} &= -\Delta t [\beta w_{ij}^{(2)} + \gamma w_{ij}^{(3)} + \mu w_{ij}^{(4)}]. \end{aligned}$$

The matrix in Eq.(15) can be written in a simplified form $\mathbf{G}\mathbf{U}^{n+1} = \mathbf{S}\mathbf{U}^n + \mathbf{L}$. (16)

Further, Eq.(16) can be rewritten as $\mathbf{G}\boldsymbol{\varepsilon}^{n+1} = \mathbf{S}\boldsymbol{\varepsilon}^n$, (17)

where: $\boldsymbol{\varepsilon}^n$ is the numerical error vector. Then Eq.(17) can be rewritten as $\boldsymbol{\varepsilon}^{n+1} = \mathbf{E}\boldsymbol{\varepsilon}^n$, $\mathbf{E} = \mathbf{G}^{-1}\mathbf{S}$.

If the eigenvalues λ_i of \mathbf{E} are distinct, then the error vector can be expanded in terms of eigenvectors \mathbf{V}^i as follows,

$$\boldsymbol{\varepsilon}^{n+1} = \sum_{i=2}^{N-1} a_i \lambda_i^{n+1} \mathbf{V}^i.$$

The stability of the proposed method is achieved when $|\lambda| \leq 1$ for all values of i as t tends to infinity. The graphs in Figs. 1 and 4 show that values $|\lambda|$ associated to the matrix \mathbf{E} are less than 1 for different grid points, indicating that the proposed scheme is unconditionally stable for the KS equation.

Similarly consider the linearized EFK equation in Eq.(13) and simplify it in the form

$$(2 + \Delta t [\mu w_{ii}^{(4)} - w_{ii}^{(2)} - 1]) U_i^{n+1} + \sum_{j=1, i \neq j}^N \Delta t [\mu w_{ij}^{(4)} - w_{ij}^{(2)}] U_j^{n+1} = (2 - \Delta t [\mu w_{ii}^{(4)} - w_{ii}^{(2)} - 1]) U_i^n - \sum_{j=1, i \neq j}^N \Delta t [\mu w_{ij}^{(4)} - w_{ij}^{(2)}] U_j^n + L_i$$

in which L_i contains the non-homogeneous part together with the boundary conditions. The above systems of linear algebraic equations are processed in the matrix form, similar as in Eq.(15), where: \mathbf{L} is a known $(N-2) \times 1$ vector and \mathbf{G} is an invertible matrix defined as

$$\begin{aligned} G_{ii} &= 2 + \Delta t [\mu w_{ii}^{(4)} - w_{ii}^{(2)} - 1], & G_{ij} &= \Delta t [\mu w_{ij}^{(4)} - w_{ij}^{(2)}] \\ S_{ii} &= 2 - \Delta t [\mu w_{ii}^{(4)} - w_{ii}^{(2)} - 1], & S_{ij} &= -\Delta t [\mu w_{ij}^{(4)} - w_{ij}^{(2)}] \end{aligned}$$

The matrix in Eq.(15) can be simplified in the same manner as in Eq.(16) for determining the stability.

NUMERICAL EXAMPLES AND ORDER OF CONVERGENCE

Different examples are solved using the proposed scheme and their accuracy is determined by evaluating error norms. Then, the order of convergence is found for both the error norms. The corresponding formulas are given as

$$\begin{aligned} L_2 &\approx \left(h \sum_{j=1}^N |U_j^{exact} - (U_N)_j| \right)^{1/2}, \\ L_\infty &\approx \max_j |U_j^{exact} - (U_N)_j|, \quad j = 1, 2, \dots, N \\ \text{Order} &= \frac{\log(\text{Error}(2N) / \text{Error}(N))}{\log(N / 2N)}, \end{aligned}$$

such that N is the number of partitions.

Example 1

The EFK equation in this example is solved on the domain $[-4, 4]$ under the conditions

$$\begin{aligned} U(x, 0) &= -\sin(\pi x), \quad x \in [-4, 4], \\ U(\pm 4, t) &= 0, \quad U_{2x}(\pm 4, t) = 0. \end{aligned}$$

The convergence rate L_2 and L_∞ errors are arranged in Table 2 and compared against results derived in /22/ and /25/, for various values of N at $t = 0.2$, $\mu = 0.1$, $\Delta t = 0.001$. The results generated by the current approach and other methods show a good degree of agreement, with second order convergence. Figures 2 and 3 are simulated for several values of μ with time t ranging from 0 to 0.2 and $N = 201$. The eigenvalues' magnitude for various grid points under the environment $\Delta t = 0.001$, $t = 0.2$ is shown in Fig. 1. Graphs involved in this figure show that the magnitude of eigenvalues \mathbf{E} are less than 1, displaying stability of the suggested method in Example 1.

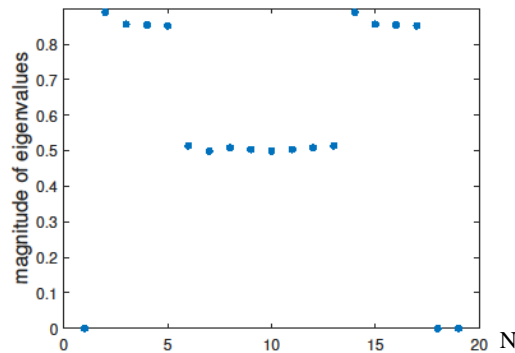


Figure 1a. Eigenvalues in example 1 at $t = 0.2$ and $N = 21$.

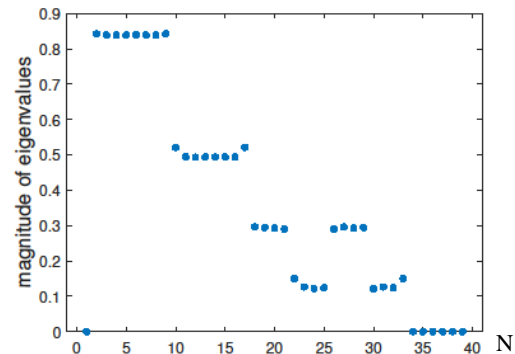


Figure 1b. Eigenvalues in example 1 at $t = 0.2$ and $N = 41$.

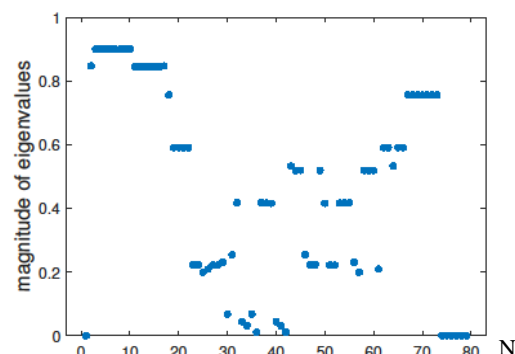


Figure 1c. Eigenvalues in example 1 at $t = 0.2$ and $N = 81$.

Table 2. Comparison of L_2, L_∞ errors and their orders of convergence in Example 1 for different values of N at $t = 0.2$.

N	Present method				Mittal and Sumita /22/				Mittal and Arora /25/			
	L_2	order	L_∞	order	L_2	order	L_∞	order	L_2	Order	L_∞	order
21	1.1412×10^{-2}		5.7836×10^{-3}		2.1347×10^{-2}		1.1547×10^{-3}		1.1158×10^{-2}		5.5097×10^{-3}	
41	2.9281×10^{-3}	2.03	1.4767×10^{-3}	2.04	2.2159×10^{-3}	2.91	1.2239×10^{-3}	3.01	2.81459×10^{-3}	2.04	1.3387×10^{-3}	2.04
81	7.4035×10^{-4}	2.02	3.7907×10^{-4}	2.00	3.12301×10^{-4}	2.82	1.5313×10^{-4}	2.93	5.6571×10^{-4}	2.1	2.8340×10^{-4}	2.23

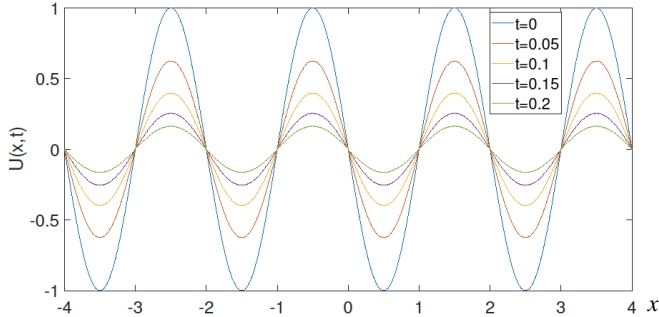


Figure 2a. $\mu = 0, \Delta t = 0.001$, and $N = 201$.

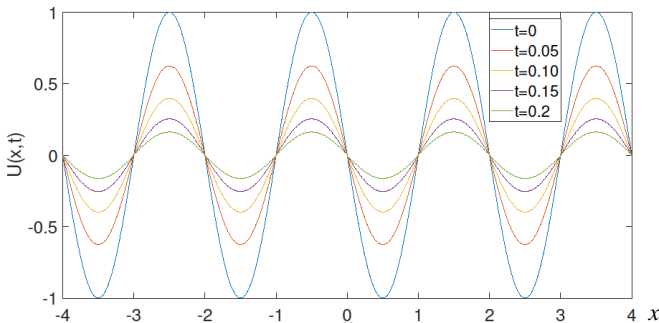


Figure 2b. $\mu = 0.0001, \Delta t = 0.001$, and $N = 201$.

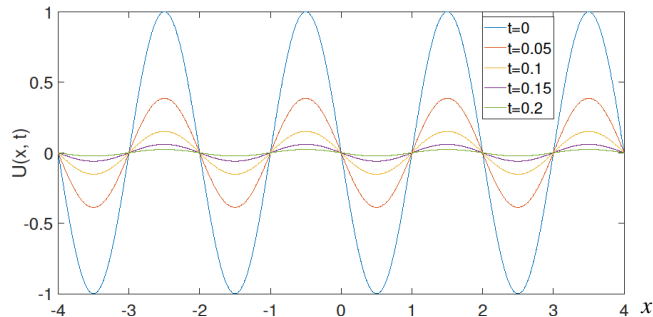


Figure 3a. $\mu = 0.1, \Delta t = 0.001$, and $N = 201$.

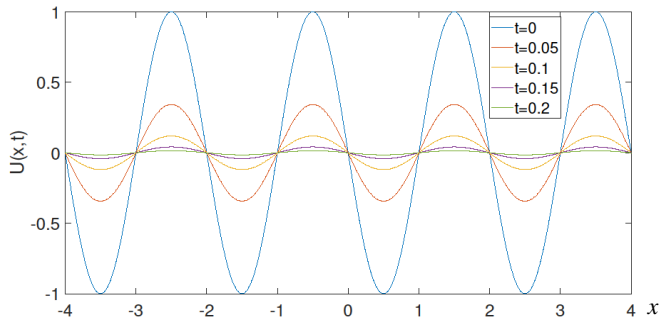


Figure 3b. $\mu = 0.125, \Delta t = 0.001$, and $N = 201$.

Example 2

Consider the EFK Eq.(2) with initial and boundary conditions

$$U(x,0) = 10^{-3} \exp(-x^2), \quad -4 \leq x \leq 4$$

$$U(\pm 4,t) = 1, \quad U_{2x}(\pm 4,t) = 0$$

The L_2, L_∞ errors along with the order of convergence for parameter $\Delta t = 0.001$ are arranged in Table 3. Data included in Table 3 reveal that the present method provides a better solution with the convergence rate of 2. The estimated solutions at different time levels with $\Delta t = 0.001$ and $N = 171$ are given in Figs. 5 and 6. It is noticeable that the approximate solution of U decreases with time and eventually converges to the value 1. Graphs in Fig. 4 display the magnitude of eigenvalues at $\Delta t = 0.001$ and $t = 4.5$ for different values of N . From the figure it is noticeable that the magnitude of eigenvalues of matrix E is smaller than 1, indicating the current method is also stable for the second example.

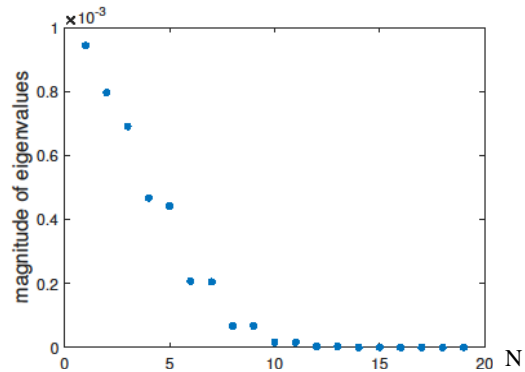


Figure 4a. Eigenvalues in example 2 at $t = 4.5$ and $N = 21$.

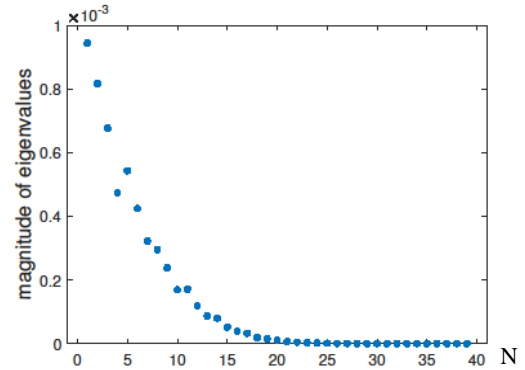


Figure 4b. Eigenvalues in example 2 at $t = 4.5$ and $N = 41$.

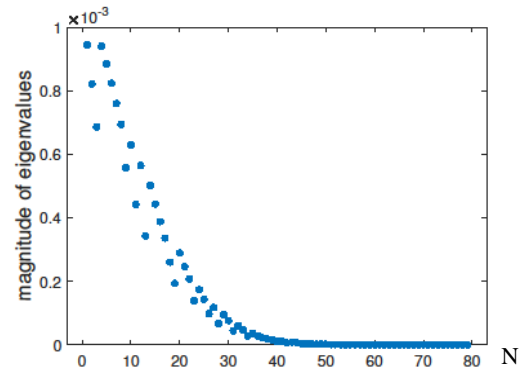


Figure 4c. Eigenvalues in example 2 at $t = 4.5$ and $N = 81$.

Table 3. Errors L_2, L_∞ with rates of convergence for various values of N in Example 2 at $t = 4.5$.

N	Present method			
	L_2	order	L_∞	order
21	3.9878×10^{-4}		2.1294×10^{-4}	
41	8.7404×10^{-5}	2.27	4.5983×10^{-5}	2.29
81	2.1910×10^{-5}	2.03	1.1528×10^{-5}	2.03

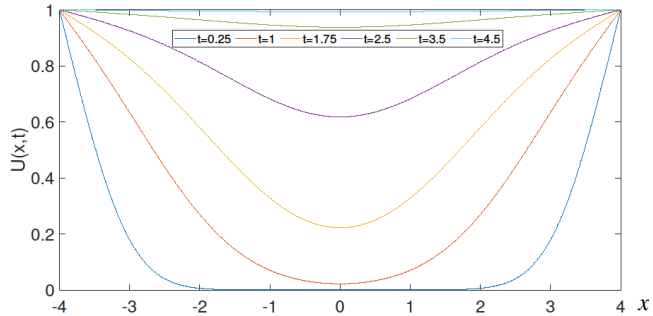


Figure 5a. $\mu = 0, \Delta t = 0.001$, and $N = 171$.

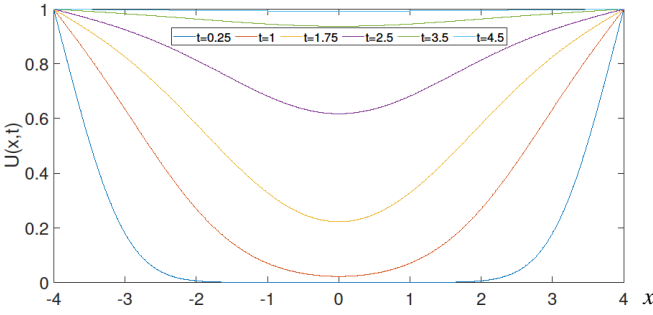


Figure 5b. $\mu = 0.0001, \Delta t = 0.001$, and $N = 171$.

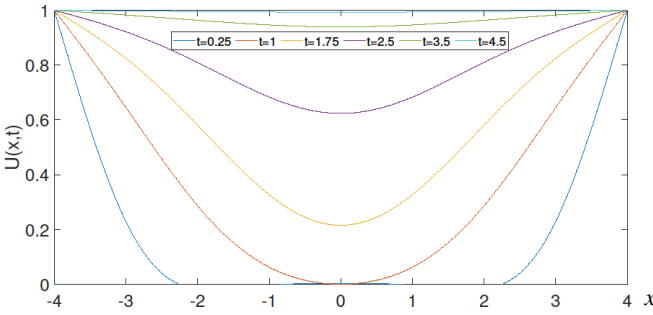


Figure 6a. $\mu = 0.1, \Delta t = 0.001$, and $N = 171$.

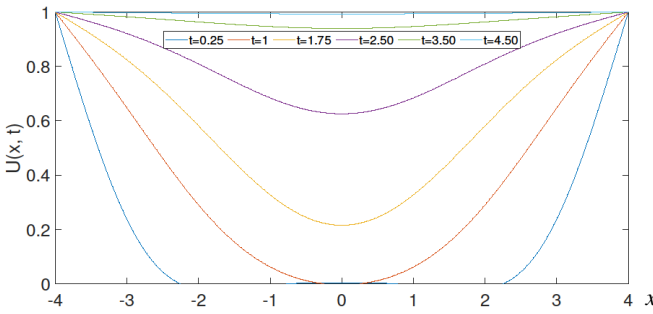


Figure 6b. $\mu = 0.120, \Delta t = 0.001$, and $N = 171$.

Example 3

The model considered in this example is the KS Eq.(3) with parameters $\alpha = \beta = \mu = 1, \gamma = 0$, under initial condition $U(x,0) = \exp(-x^2), x \in [-30,30]$ and boundary condition $U(\pm 30,t) = 0$.

Graphs plotted in Figs. 8 and 9 give a representation of the numerical solution for $t = 1, 5, 10, 20$ at $\Delta t = 0.001$ and $N = 201$. These graphs exhibit the same characteristics as in /23/. The magnitude of eigenvalues for $\Delta t = 0.001$ at $t = 20$ is shown in Fig. 7 for different values of N . The suggested approach is stable for Example 3, as shown by this graph, in which eigenvalue magnitudes for various values of N remain less than 1.

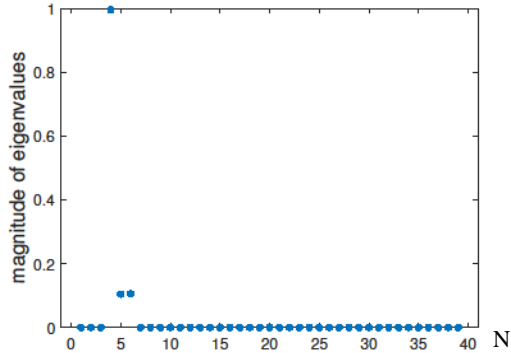


Figure 7a. Eigenvalues in example 3 at $t = 20$ and $N = 41$.

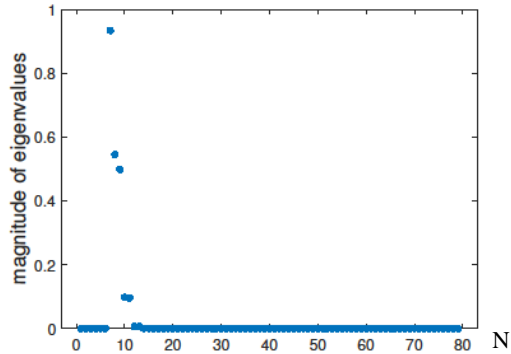


Figure 7b. Eigenvalues in example 3 at $t = 20$ and $N = 81$.

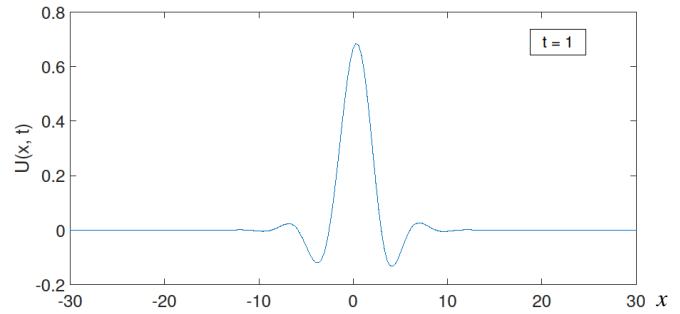


Figure 8a. $t = 1, \Delta t = 0.001$, and $N = 201$.

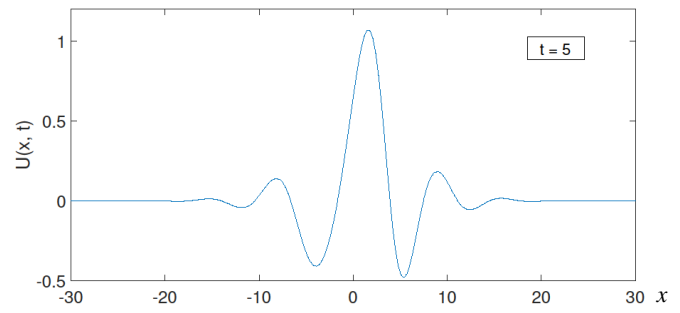


Figure 8b. $t = 5, \Delta t = 0.001$, and $N = 201$.

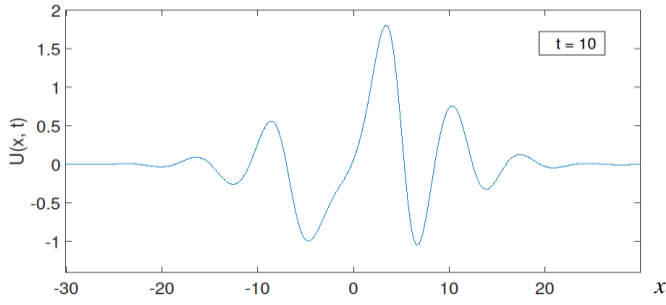


Figure 9a. $t = 10$, $\Delta t = 0.001$, and $N = 201$.

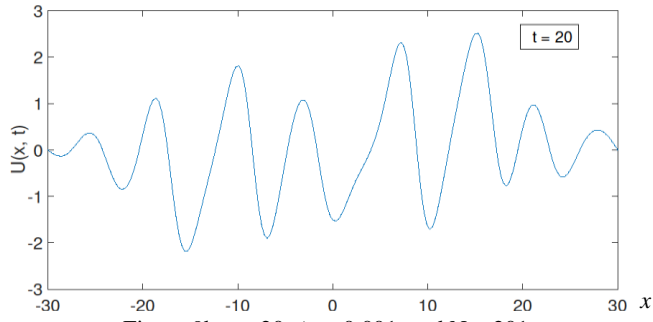


Figure 9b. $t = 20$, $\Delta t = 0.001$, and $N = 201$.

Example 4

In this example, the KS Eq.(3) is solved for parameters $\alpha = \beta = 1$, $\gamma = 0$, for various values of μ , and with the following conditions in the domain $[-1, 1]$:

$$U(x,0) = -\sin(\pi x), \quad x \in [-1, 1], \quad U(\pm 1, t) = 0.$$

Figures 11 and 12 are plotted for values of $\mu = 0.4/(\pi^2)$, $\mu = 0.8/(\pi^2)$, and $\mu = 1.2/(\pi^2)$ at different time levels. These graphs exhibit the same behaviour as in /24/. In Fig. 10, the magnitude of eigenvalues is plotted for different values of N with $\Delta t = 0.001$ and $t = 2$. It is obvious that the magnitude of eigenvalues E is less than 1, displaying that the present method is stable in Example 4.

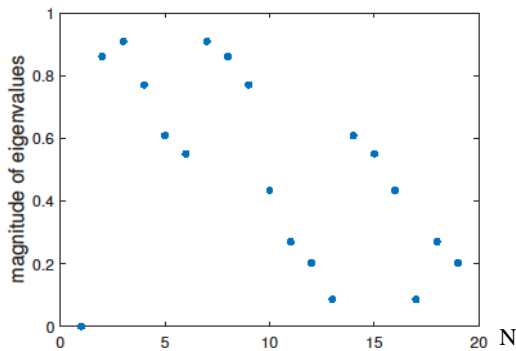


Figure 10a. Eigenvalues in example 4 at $t = 2$ and $N = 21$.

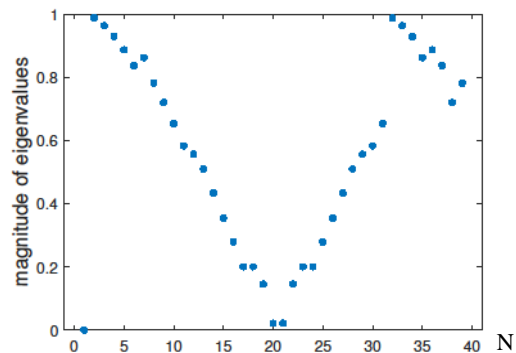


Figure 10b. Eigenvalues in example 4 at $t = 2$ and $N = 41$.

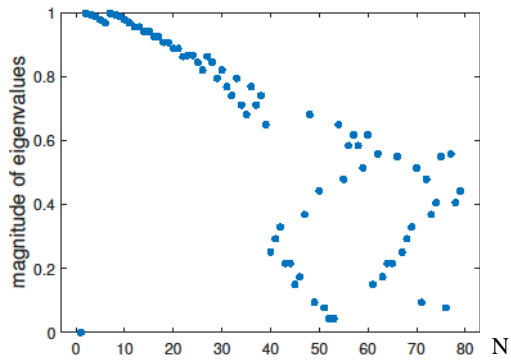


Figure 10c. Eigenvalues in example 4 at $t = 2$ and $N = 81$.

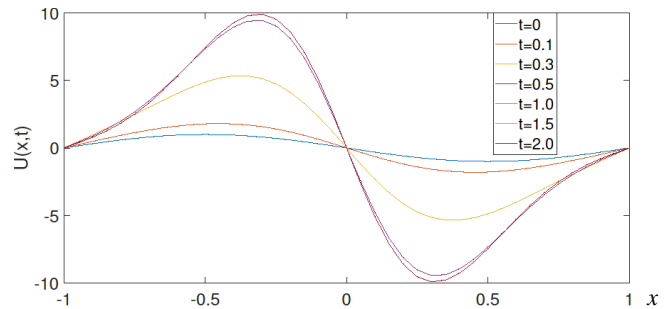


Figure 11a. $\mu = 0.4/\pi^2$, $\Delta t = 0.001$ and $N = 41$.

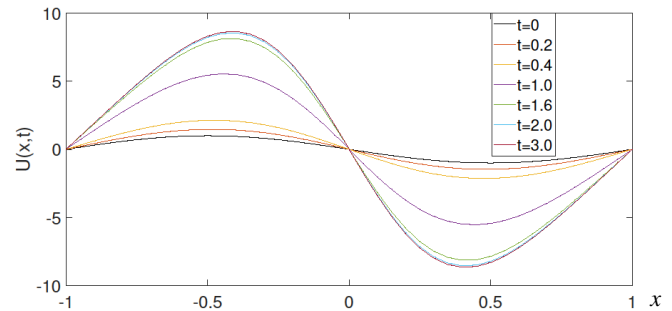


Figure 11b. $\mu = 0.8/\pi^2$, $\Delta t = 0.001$ and $N = 41$.

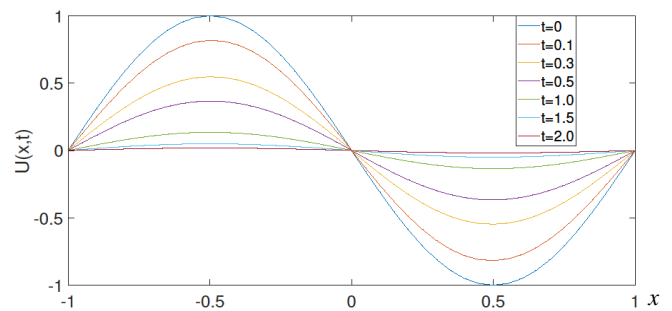


Figure 12. $\mu = 1.2/\pi^2$, $\Delta t = 0.001$ and $N = 41$.

CONCLUSION

This work proposes a modified quintic B-spline based differential quadrature method to obtain the numerical solution of the nonlinear generalised Kuramoto-Sivashinsky (GKS) equation. Two reduced forms of the GKS equation are considered, namely extended Fisher-Kolmogorov equation and Kuramoto-Sivashinsky equation. Stability is examined using matrix stability analysis, and unconditional stability is confirmed. Four numerical problems are studied to verify theoretical results and to bolster the significance of the method. Through numerical data arranged in tables and plotted graphs it is perceptible that obtained numerical results

are better than the solutions available in literature. In summary, various classes of nonlinear differential equations can be solved using modified quintic B-spline based DQM owing to its accuracy and computational efficiency.

ACKNOWLEDGEMENTS

Predrag Stanimirović is supported by the Ministry of Science, Technological Development and Innovation, of the Republic of Serbia, Contract No. 451-03-65/2024-03/200124.

REFERENCES

- Akrivis, G., Smyrlis, Y.-S. (2004), *Implicit-explicit BDF methods for the Kuramoto-Sivashinsky equation*, Appl. Num. Math. 51 (2-3): 151-169. doi: 10.1016/j.apnum.2004.03.002
- Başhan, A. (2021), *Modification of quintic B-spline differential quadrature method to nonlinear Korteweg-de Vries equation and numerical experiments*, Appl. Num. Math. 167: 356-374. doi: 10.1016/j.apnum.2021.05.015
- Bellman, R., Kashef, B.G., Casti, J. (1972), *Differential quadrature: A technique for the rapid solution of nonlinear partial differential equations*, J Comput. Phys. 10(1): 40-52. doi: 10.1016/0021-9991(72)90089-7
- Bellman, R., Kashef, B., Lee, E.S., Vasudevan, R. (1975), *Differential quadrature and splines*, Comp. Math. Appl. 1(3-4): 371-376. doi: 10.1016/0898-1221(75)90038-3
- Benguria, R.D., Depassier, M.C. (2005), *On the transition from pulled to pushed monotonic fronts of the extended Fisher-Kolmogorov equation*, Phys. A: Stat. Mech. Appl. 356(1): 61-65. doi: 10.1016/j.physa.2005.05.013
- Bhatia, R., Mittal, R.C. (2018), *Numerical study of Schrödinger equation using differential quadrature method*, Int. J Appl. Comput. Math. 4: 36. doi: 10.1007/s40819-017-0470-x
- Coulet, P., Elphick, C., Repaux, D. (1987), *Nature of spatial chaos*, Phys. Rev. Lett. 58: 431-434. doi: 10.1103/PhysRevLett.58.431
- Cueto-Felgueroso, L., Peraire, J. (2008), *A time-adaptive finite volume method for the Cahn-Hilliard and Kuramoto-Sivashinsky equations*, J Comput. Phys. 227(24): 9985-10017. doi: 10.1016/j.jcp.2008.07.024
- Dabboura, E., Sadat, H., Prax, C. (2016), *A moving least squares meshless method for solving the generalized Kuramoto Sivashinsky equation*, Alexandria Eng. J. 55(3): 2783-2787. doi: 10.1016/j.aej.2016.07.024
- Dee, G.T., van Saarloos, W. (1988), *Bistable systems with propagating fronts leading to pattern formation*, Phys. Rev. Lett. 60: 2641-2644. doi: 10.1103/PhysRevLett.60.2641
- Gudi, T., Gupta, H.S. (2013), *A fully discrete C^0 interior penalty Galerkin approximation of the extended Fisher-Kolmogorov equation*, J Comput. Appl. Math. 247: 1-16. doi: 10.1016/j.cam.2012.12.019
- Haq, S., Bibi, N., Tirmizi, S.I.A., Usman, M. (2010), *Meshless method of lines for the numerical solution of generalized Kuramoto-Sivashinsky equation*, Appl. Math. Comput. 217(6): 2404-2413. doi: 10.1016/j.amc.2010.07.041
- Hepson, O.E., Yigit, G. (2022), *A numerical scheme for the wave simulations of the Kuramoto-Sivashinsky model via quartic-trigonometric tension B-spline*, Wave Motion, 114: 103045. doi: 10.1016/j.wavemoti.2022.103045
- Ismail, K., Atouani, N., Omrani, K. (2022), *A three-level linearized high-order accuracy difference scheme for the extended Fisher-Kolmogorov equation*, Eng. Comp. 38(suppl.2): 1215-1225. doi: 10.1007/s00366-020-01269-4
- Jain, M.K., Numerical Solution of Differential Equations, 2nd Ed., John Wiley & Sons, New York, 1983.
- Khater, A.H., Temsah, R.S. (2008), *Numerical solutions of the generalized Kuramoto-Sivashinsky equation by Chebyshev spectral collocation methods*, Comp. Math. Appl. 56(6): 1465-1472. doi: 10.1016/j.camwa.2008.03.013
- Lai, H., Ma, C. (2009), *Lattice Boltzmann method for the generalized Kuramoto-Sivashinsky equation*, Phys. A: Statist. Mech. Appl. 388(8): 1405-1412. doi: 10.1016/j.physa.2009.01.005
- Lakestani, M., Dehghan, M. (2012), *Numerical solutions of the generalized Kuramoto-Sivashinsky equation using B-spline functions*, Appl. Math. Model. 36(2): 605-617. doi: 10.1016/j.am.2011.07.028
- Mittal, R.C., Bhatia, R. (2013), *Numerical solution of second order one dimensional hyperbolic telegraph equation by cubic B-spline collocation method*, Appl. Math. Comput. 220: 496-506. doi: 10.1016/j.amc.2013.05.081
- Mittal, R.C., Bhatia, R. (2015), *Numerical solution of nonlinear system of Klein-Gordon equations by cubic B-spline collocation method*, Int. J Comp. Math. 92(10): 2139-2159. doi: 10.1080/0207160.2014.970182
- Mittal, R.C., Bhatia, R. (2014), *A numerical study of two dimensional hyperbolic telegraph equation by modified B-spline differential quadrature method*, Appl. Math. Comput. 244: 976-997. doi: 10.1016/j.amc.2014.07.060
- Mittal, R.C., Dahiya, S. (2016), *A study of quintic B-spline based differential quadrature method for a class of semi-linear Fisher-Kolmogorov equations*, Alexandria Eng. J. 55(3): 2893-2899. doi: 10.1016/j.aej.2016.06.019
- Mittal, R.C., Dahiya, S. (2017), *A quintic B-spline based differential quadrature method for numerical solution of Kuramoto-Sivashinsky equation*, Int. J Nonlin. Sci. Num. Simul. 18(2): 103-114. doi: 10.1515/ijnsns-2015-0190
- Mittal, R.C., Arora, G. (2010), *Quintic B-spline collocation method for numerical solution of the Kuramoto-Sivashinsky equation*, Comm. Nonlin. Sci. Num. Simul. 15(10): 2798-2808. doi: 10.1016/j.cnsns.2009.11.012
- Mittal, R.C., Arora, G. (2010), *Quintic B-spline collocation method for numerical solution of the extended Fisher-Kolmogorov equation*, Int. J Appl. Math. Mech. 6(1): 74-85.
- Peletier, L.A., Troy, W.C. (1995), *A topological shooting method and the existence of kinks of the extended Fisher-Kolmogorov equation*, Topol. Methods Nonlin. Anal. 6(2): 331-355.
- Peletier, L.A., Troy, W.C. (1996), *Chaotic spatial patterns described by the extended Fisher-Kolmogorov equation*, J Differ. Equat. 129(2): 458-508. doi: 10.1006/jdeq.1996.0124
- Quan, J.R., Chang, C.T. (1989), *New insights in solving distributed system equations by the quadrature method-II, Numerical experiments*, Comp. Chem. Eng. 13(9): 1017-1024. doi: 10.1016/0098-1354(89)87043-7
- Quan, J.R., Chang, C.T. (1989), *New insights in solving distributed system equations by the quadrature method-I. Analysis*, Comp. Chem. Eng. 13(7): 779-788. doi: 10.1016/0098-1354(89)85051-3
- Wazzan, L. (2009), *Modified tanh-coth method for solving the general Burgers-Fisher and the Kuramoto-Sivashinsky equations*, Comm. Nonlin. Sci. Num. Simul. 14(6): 2642-2652. doi: 10.1016/j.cnsns.2008.08.004
- Xu, Y., Shu, C.-W. (2006), *Local discontinuous Galerkin methods for the Kuramoto-Sivashinsky equations and the Ito-type coupled KdV equations*, Comp. Meth. Appl. Mech. Eng. 195(25-28): 3430-3447. doi: 10.1016/j.cma.2005.06.021
- Zuo, J. (2022), *New compact finite difference schemes with fourth-order accuracy for the extended Fisher-Kolmogorov equation*, Eng. Lett. 30(1): 1-15.

© 2025 The Author. Structural Integrity and Life, Published by DIVK (The Society for Structural Integrity and Life 'Prof. Dr Stojan Sedmak') (<http://divk.inovacionicentar.rs/ivk/home.html>). This is an open access article distributed under the terms and conditions of the Creative Commons Attribution-NonCommercial-NoDerivatives 4.0 International License